High excited states of magnetodonors in InSb: An experimental and theoretical study

W. Zawadzki,* X. N. Song, and C. L. Littler
Department of Physics, University of North Texas, P.O. Box 5368, North Texas Station, Denton, Texas 76203-5368

D. G. Seiler
Semiconductor Electronics Division, National Institute of Standards and Technology, Gaithersburg, Maryland 20899
(Received 13 April 1990)

New optical transitions between magnetodonor states in InSb assisted by optic-phonon emission have been observed and described theoretically. Photoconductive detection and magnetic-field modulation were used to obtain well-resolved magneto-optical data. Phonon-assisted excitations provide a unique opportunity to investigate high excited states of the magnetodonor system (up to principal quantum number $n=13$), which simulates the hydrogen atom in gigantic magnetic fields. The magnetodonor states have been described variationally, taking into account the narrow energy gap and the spin-orbit interaction of the band structure of InSb. It has been shown how the phonon emission breaks the selection rules for the magneto-optical excitations, allowing for transitions with large Δn. Good agreement between theory and experiment has been obtained. The results should also be of importance to atomic physics and astrophysics.

I. INTRODUCTION

Magnetodonor (MD) states in semiconductors, since their discovery in the magnetic freeze-out effect by Keyes and Sladek[1] and the pioneering theoretical description of Yafet, Keyes, and Adams,[2] have been the subject of sustained experimental and theoretical interest. The effect of a magnetic field on shallow donor states is particularly important in narrow-band-gap materials with small effective masses m^* since, in the absence of the field, the donors are ionized even at low temperatures and cannot be observed. Important progress in the magneto-optical investigations of shallow donor states was achieved by Kaplan,[3] who used the photoconductive detection technique to observe both low-energy transitions between MD states belonging to the same Landau subband, as well as those occurring between MD states belonging to adjacent Landau subbands. The latter is sometimes referred to as "donor-shifted cyclotron resonance." Similar MD transitions related to spin resonance[4] and combined cyclotron-spin resonance[5] have also been observed in InSb. Magnetodonor investigations have been used to determine the static dielectric constant of a material[6] and its pressure dependence,[7] to identify the chemical nature of impurities,[8] to study screening properties of the electron gas,[9] to investigate the metal-nonmetal transition,[10] etc. Recently, magneto-optical and magnetotransport investigations proved to be useful in determining the positions of donors in modulation-doped two-dimensional GaAs-$Ga_{1-x}Al_xAs$ structures,[11,12] which is important for device applications.

The importance of the magnetodonor system goes beyond semiconductor physics, however, since a magnetodonor imitates the hydrogen atom in giant magnetic fields. The problem of an electron subjected to simultaneous Coulomb and magnetic field interactions is characterized by the parameter $\gamma=(\hbar eB/m^*)/(2\,\mathrm{Ry}^*)$, where $\mathrm{Ry}^*\equiv 13.6(m^*/m_0)/\kappa_0^2$ eV, and κ_0 is the static dielectric constant. The value of γ is of the order of 10^{-5} for the hydrogen atom in vacuum. In narrow-band-gap semiconductors, however, γ can attain values of 100 or more for available magnetic field strengths. In our experiments we deal typically with $\gamma\simeq 25$, which corresponds to the hydrogen atom in a vacuum subjected to a magnetic field of $\simeq 10^7$ T. The above scaling allows one to transpose magnetodonor behavior to that of the hydrogen atom in gigantic magnetic fields.

The problem of atoms in extremely large magnetic fields has attracted a great deal of attention in recent years both in atomic physics and astrophysics.[13] The reason is that white dwarf stars can produce magnetic fields of 10^3 T and accreting neutron star fields of the order of 10^6–10^8 T. As a consequence, the optical spectra of atoms in such magnetic fields have been observed in the spectra of these stars. For example, very good agreement between all observed spectral features and the computed wavelengths of stationary transitions of the hydrogen atom in magnetic fields $(1.5-3.5)\times 10^4$ T has been found in the white dwarf GrW+70°8L47.[14] By virtue of scaling laws the energies of heavier atoms can also be estimated from those of the hydrogen atom at scaled values of magnetic field.[15] This allows one to study, for example, Fe XXVI in gigantic fields, which appears to be prevailing in the vicinity of x-ray pulsars.[16] The ionization thresholds of the hydrogen atom associated with higher Landau levels are of current interest in astrophysical investigations.[17]

The importance of the magneto-Coulomb system in astrophysics and atomic physics has motivated considerable theoretical work concerned with the behavior of the hydrogen atom at arbitrary magnetic fields (cf. Rösner *et al.*[18]). The corresponding theoretical work related to magnetodonors and magnetoacceptors has been reviewed by Zawadzki.[19] Magneto-optical transitions in semicon-

ductors with a change in the Landau quantum number $\Delta n=2$ and $\Delta n=3$ are possible due to the intricacies of the band structure, such as warping and the lack of inversion symmetry,[20,21] and they have been observed in InSb.[20,22] The corresponding donor-shifted resonances have been observed by Grisar *et al.*[20] The effect of optic phonons on free-electron transitions between Landau levels (breaking of the selection rules) has been predicted by Bass and Levinson[23] and first observed by Enck *et al.*[24] Transitions to very high Landau states (up to $n=23$) have been seen by Goodwin and Seiler.[25] Phonon-assisted spin-flip transitions have been observed and described by Zawadzki *et al.*[26] The effect of optic phonons on optical transitions between MD states has been observed by Kaplan and Wallis[27] in the form of resonant polaron behavior in donor-shifted cyclotron resonance, and by McCombe and Wagner[5] in donor-shifted combined resonance.

In this paper we report on a new kind of optical transition between MD states assisted by the emission of optic phonons.[28] Indirect evidence for such transitions was provided by Huant *et al.*[29] and Littler and Seiler.[30] In Sec. II we describe the experimental procedure, Sec. III contains the magnetodonor theory, and in Sec. IV we present our results and discuss them.

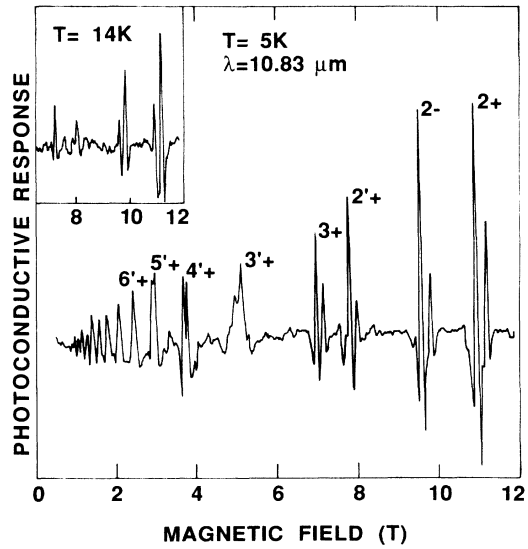

FIG. 1. Photoconductive response of n-type InSb vs magnetic field obtained at 5 K using a CO_2 laser wavelength of 10.83 μm (second derivative with respect to magnetic field). The final Landau states are indicated. The primes refer to phonon-assisted transitions. The inset shows a magneto-optical spectrum obtained at a higher temperature.

II. EXPERIMENTAL PROCEDURE

The experiments were performed on high-purity samples of n-type InSb with a carrier concentration of 9×10^{13} cm^{-3} and an electron mobility of 7×10^5 cm^2/V sec at 77 K. The samples were rectangular slabs whose surfaces were lapped using alumina grit and then chemically etched using a 2% bromine–methanol solution. Electrical contacts were made to the samples using pure indium. The output of a grating tunable cw CO_2 laser was mechanically chopped into 20-μsec-wide pulses with a low duty cycle to prevent lattice-heating effects. The laser radiation was focused onto a sample situated in the solenoid of a superconducting magnet capable of producing dc magnetic fields as high as 12 T. For all measurements reported here the Faraday configuration was used. The magnet contains modulation coils which are used to impress a small (±0.1 T) ac magnetic field on the larger dc field. Boxcar averaging and lock-in amplifier techniques are then employed to obtain derivative-like spectra.[31] Photoconductive measurements were used to provide a sensitive means of detecting small changes in absorption.[3] All spectra shown in this work represent the second derivative of the photoconductive response versus magnetic field.

In Fig. 1 we show the photoconductivity spectra obtained with the use of the above technique. As explained below, the doublet structure is related to optical transitions between Landau levels accompanied by corresponding transitions between magnetodonor states. By increasing the temperature (cf. inset Fig. 1), we increase the occupancy of the free-electron ground state, thus enhancing the free-electron transitions (cf. inset Fig. 5).

III. THEORY

A. Effective-mass approximation

In order to define all quantities and to stress the analogy between the magnetodonor and the hydrogen atom in a magnetic field, we first consider the one-band effective-mass approximation (cf. Ref. 2). The initial MD Hamiltonian reads (neglecting spin),

$$H=\frac{1}{2m_0^*}(\mathbf{p}+e\,\mathbf{A})^2-\frac{e^2}{\kappa_0 r}\ , \tag{1}$$

where curl $\mathbf{A}=\mathbf{B}$ is the magnetic field (we take $\mathbf{B}\|\mathbf{z}$). The effective mass m_0^* and the static dielectric constant κ_0 account for the presence of the semiconducting medium. Using the symmetric gauge $\mathbf{A}=(-By/2,Bx/2,0)$, the Hamiltonian becomes

$$H=\frac{p^2}{2m_0^*}+\tfrac{1}{2}\hbar\omega_c L_z+\tfrac{1}{8}m_0^*\omega_c^2(x^2+y^2)-\frac{e^2}{\kappa_0 r}\ , \tag{2}$$

where $\omega_c=eB/m_0^*$ is the cyclotron frequency and $\hbar L_z=(xp_y-yp_x)$. Introducing the effective Rydberg $\mathrm{Ry}^*\equiv m_0^*e^4/2\hbar^2\kappa_0^2$ as a unit of energy, and the effective Bohr radius $a_B^*=\kappa_0\hbar^2/m_0^*e^2$ as a unit of length, one obtains

$$H=-\nabla^2+\gamma L_z+\frac{\gamma^2}{4}(x^2+y^2)-\frac{2}{r}\ \mathrm{Ry}^*\ , \tag{3}$$

where x, y, z, and r are dimensionless. The characteristic parameter

$$\gamma=\frac{\hbar\omega_c}{2\ \mathrm{Ry}^*}=\left[\frac{a_B^*}{L}\right]^2 \tag{4}$$

measures the relative strength of the magnetic and the Coulomb interactions. The magnetic length is $L=\sqrt{\hbar/eb}$.

Expressed in the dimensionless quantities (3) and (4), the Hamiltonians for the magnetodonor and the hydrogen atom in a magnetic field have the same form, which depends on γ as the only parameter. However, the values of γ in the two cases are usually very different. For the hydrogen atom in a magnetic field of $B=10$ T, one has $\gamma\simeq 3\times 10^{-5}$, which is the regime of the Zeeman effect. On the other hand, in semiconductors the values of $\gamma>10$ can be achieved due to small effective masses and large dielectric constants. In this situation it is not possible to treat the magnetic interaction as a perturbation. There have been three ways to treat the problem for arbitrary γ: (1) the variational procedure, (2) the adiabatic approximation (based on a separation of the transverse and parallel motions at high magnetic fields), and (3) expansion techniques (in which the wave function is expanded in a set of known functions). These methods have been reviewed in Ref. 19. We use the variational procedure, which can be directly generalized for the case of narrow-band-gap semiconductors.

B. Three-level P·p model

Since InSb is a narrow band-gap semiconductor, the intricacies of its band structure, i.e., the proximity of the valence band and the spin-orbit interaction, have to be incorporated into the calculation of both the conduction-electron energies in the presence of a magnetic field and the corresponding MD binding energies. We have calculated the Landau energies of the conduction electrons using a spherical version of the Pidgeon and Brown model.[32] This model takes explicitly into account the Γ_6^c, Γ_8^v, and Γ_7^v bands, incorporating all other bands in the k^2 approximation. In this procedure the calculation of eigenvalues amounts to a diagonalization of two 4×4 matrices, for the spin-up and spin-down states. In Sec. IV we quote the corresponding band parameters used.

In order to account for the influence of the band structure on the MD energies we use a somewhat simpler description known as the three-level model (cf. Refs, 33 and 34). It incorporates explicitly the Γ_6^c, Γ_8^v, and Γ_7^v bands, neglecting the influence of all other bands. The initial Hamiltonian for our problem reads

$$H=\frac{1}{2m_0}P^2+V_0(\mathbf{r})+\frac{\hbar}{4m_0^2c^2}(\boldsymbol{\sigma}\times\nabla V_0)\cdot\mathbf{P}+\mu_B\mathbf{B}\cdot\boldsymbol{\sigma}+U(\mathbf{r}) , \tag{5}$$

where $\mathbf{P}=\mathbf{p}+e\mathbf{A}$, the spin-orbit and Pauli terms are written in the standard notation, V_0 is the periodic potential of the lattice, and

$$U(\mathbf{r})=-e^2/\kappa_0 r \tag{6}$$

is the donor (slowly varying) potential. One looks for solutions of the eigenenergy problem in the form

$$\psi(\mathbf{r})=\sum_l f_l(\mathbf{r})u_l(\mathbf{r}) , \tag{7}$$

where the summation runs over the energy bands, f_l are the slowly varying envelope functions, and u_l are the Luttinger-Kohn periodic amplitudes satisfying the band-edge eigenenergy equation

$$\left[\frac{1}{2m_0}P^2+V_0+H_{\text{s.o.}}\right]u_l=\varepsilon_{l0}u_l , \tag{8}$$

where ε_{l0} is the edge energy for the lth band. Inserting (7) into (5) and using (8) one obtains

$$\sum_l\left[\left[-E+\frac{1}{2m_0}P^2+\varepsilon_{l0}+U\right]\delta_{l'l}+\frac{1}{m_0}\mathbf{p}_{l'l}\cdot\mathbf{P}+\mu_B\mathbf{B}\cdot\boldsymbol{\sigma}_{l'l}\right]f_l=0 , \tag{9}$$

where $l'=1,2,3,\ldots$ and

$$\mathbf{p}_{l'l}=\left\langle u_{l'}\left|\mathbf{p}+\frac{\hbar}{4m_0c^2}(\boldsymbol{\sigma}\times\nabla V_0)\right|u_l\right\rangle . \tag{10}$$

Specifying the periodic Luttinger-Kohn functions for the three levels in question and neglecting all other bands, the infinite set (9) reduces to eight coupled differential equations. We neglect in addition the orbital and spin free-electron terms since they give very small contributions for narrow-band-gap-materials. The resulting set can be solved by substitution, expressing the $f_3,f_4,\ldots,f_8$ functions in terms of f_1 and f_2. The result is

$$[-(E-U)(E-U+\varepsilon_g)(E-U+\varepsilon_g+\Delta)+\kappa^2(E-U+\varepsilon_g+\tfrac{2}{3}\Delta)P^2\pm\tfrac{1}{3}\kappa^2\hbar eB\Delta]\times\begin{Bmatrix}f_2\\f_1\end{Bmatrix}=\begin{Bmatrix}0\\0\end{Bmatrix} , \tag{11}$$

where $\kappa=-(i/m_0)\langle S|p_x|X\rangle$ is the interband matrix element of momentum and Δ is the spin-orbit energy. The plus and minus signs correspond to spin-down and spin-up state, respectively. Equation (11) presents a generalization of the equations of Kanes[35] and Bowers and Yafet[36] for conduction electrons in the simultaneous presence of a magnetic field and an electric potential. To arrive at the form (11) we have neglected the commutators $[\mathbf{p}, U]$. They give rise to small corrections to the energies (cf. Ref. 33), but are negligible for our purpose.

One can now use the variational procedure on the effective equations given in (11) which, apart from the above simplifications, accounts for the intricacies of the InSb band structure. If $E-\langle U\rangle\ll\varepsilon_g+2\Delta/3$, which is

the case for InSb, one can neglect the corresponding terms in Eq. (11) and solve the resulting quadratic equation for the energies. We obtain for the conduction band (in Ry* units)

$$E_{\mp}=-\frac{\varepsilon_g}{2}+\left[\left[\frac{\varepsilon_g}{2}\right]^2+\varepsilon_g\left[\langle K\rangle\pm\gamma\frac{\Delta}{2\Delta+3\varepsilon_g}\right]\right]^{1/2}+\langle U\rangle\ , \tag{12}$$

where

$$K=-\nabla^2-i\gamma\frac{\partial}{\partial\phi}+\frac{\gamma^2\rho^2}{4} \tag{13}$$

and the last term under the square root gives the effective spin splitting. The quantities $\langle K\rangle$ and $\langle U\rangle$ are variational averages of the kinetic energy (13) and potential energy $U=-2/(\rho^2+z^2)^{1/2}$ (in cylindrical coordinates), respectively. The energy gap ε_g and the spin-orbit energy Δ in (12) should be expressed in Ry* units. The effective mass at the band edge resulting from the above theory is

$$\frac{1}{m_0^*}=\tfrac{2}{3}\kappa^2\frac{2\Delta+3\varepsilon_g}{\varepsilon_g(\Delta+\varepsilon_g)}\ . \tag{14}$$

In practice one takes the experimental values for m_0^* and the spin-splitting factor g_0^*. Thus the evaluation of the MD energy amounts to the calculation of the trial averages $\langle K\rangle$ and $\langle U\rangle$ for a given state and a minimization of the energy given in (12).

C. Magnetodonor energies

Following Ref. 34, we choose the two-parameter trial functions in the form (cylindrical coordinates),

$$f_{NM\beta}=A_{NM}e^{iM\phi}\eta^{|m|/2}e^{-\eta/2}L_N^m(\eta)P_\beta(zb)\ , \tag{15}$$

where N, M, and β are the quantum numbers, $\eta=\gamma\rho^2a^2/2$, the normalization factor for the (ρ,ϕ) part is $A_{NM}=[\gamma N!a^2/(N+M)!2\pi]^{1/2}$, a is the first variational parameter, L_N^m are the associated Laguerre polynomials, and $m=|M|$. The variables ρ and z are dimensionless (in units of a_B^*). The quantum numbers can take the following values: $N=0,1,2,\ldots$; $M=\ldots,-2,-1,0,1,2,\ldots$; $\beta=0,1,2,\ldots$. The z parts of the trial functions for $\beta=0$ and $\beta=1$ are

$$P_0=\left[\frac{\gamma b^2}{2\pi}\right]^{1/4}e^{-\gamma b^2z^2/4}\ , \tag{16}$$

and

$$P_1=\left[\frac{\gamma^3b^6}{2\pi}\right]^{1/4}ze^{-\gamma b^2z^2/4}\ , \tag{17}$$

where b is the second variational parameter. The function $P(z)$ for $\beta=2$ can be found in Refs. 34 and 37.

The above functions are generalizations of the Yafet-Keyes-Adams[2] ground state ψ_{000}. For large γ values a MD state described by $NM\beta$ "belongs" to the Landau subband described by the quantum number $n=N+(M+m)/2$, i.e., its energy is somewhat lower than the nth Landau level. Thus, at high fields one deals with "ladders" of MD states "attached" to each Landau subband. The ladders arise due to different β values and from the fact that the Coulomb potential lifts the degeneracy of the Landau levels related to the N and M values. Using the above variational functions one can now calculate trial integrals for the kinetic and potential energies. The kinetic-energy integrals are best done in cylindrical coordinates, while the potential-energy integrals are best done in spherical coordinates. For arbitrary N, M, and $\beta=0,1$ one arrives at the following expressions:[34]

$$\langle K\rangle=\frac{\gamma}{2}(2N+m+1)\left[\frac{\epsilon}{\lambda}+\frac{\lambda}{\epsilon}\right]+\gamma M+\gamma\lambda\frac{2\beta+1}{4}\ , \tag{18}$$

$$\langle U\rangle=-2\frac{N!(N+m)!}{(2N+m)!\,\Gamma(2N+\frac{1}{2})}\left[\frac{\gamma\lambda}{2\pi}\right]^{1/2}(-2\epsilon)^\beta\times\frac{d^\beta}{d\epsilon^\beta}\left\{(1-\epsilon)^{-m}\sum_{j=0}^{N}\frac{\Gamma(2N-2j+\frac{1}{2})}{j![(N-j)!]^2(m+j)!}\frac{d^{2j}}{d\epsilon^{2j}}\left[(1-\epsilon)^{m+2j}\frac{d^m}{d\epsilon^m}\left[\epsilon^{2N+m}\frac{d^{2N}}{d\epsilon^{2N}}\frac{D(\epsilon)}{(1-\epsilon)^{1/2}}\right]\right]\right\}\ , \tag{19}$$

where $\lambda=b^2$ and $\epsilon=b^2/a^2$ are new variational parameters, and

$$D(\epsilon)=\ln\left[\frac{1+\sqrt{1-\epsilon}}{1-\sqrt{1-\epsilon}}\right]\ . \tag{20}$$

The expressions for $\beta=2$ can be found in Refs. 34 and 37.

In our experiments on InSb we deal typically with the values of $\gamma>30$. In this case the transverse motion is controlled by the magnetic field and the transverse MD radius becomes equal to the radius L (cf. Ref. 2). In our notation this means $a^2=1$ and $\epsilon=\lambda$. This is equivalent to using the one-parameter trial wave functions first proposed by Wallis and Bowlden.[37] The above expressions for the sum $\langle K\rangle+\langle U\rangle$ should then be equivalent to the corresponding expressions of Ref. 37, since the same trial functions are used. This is indeed the case, although the

verification of this equivalence requires some manipulations.

Equation (19) becomes particularly simple for the $(0m0)$ states, which belong to the corresponding $n=m$ Landau subbands. We have

$$\langle K\rangle_{0m0}=\gamma(2m+1)+\tfrac{1}{4}\gamma\lambda \text{ Ry}^* \tag{21}$$

and

$$\langle V\rangle_{0m0}=-\frac{2}{m!}\left[\frac{\gamma\lambda}{2\pi}\right]^{1/2}\frac{d^m}{d\lambda^m}\left[\lambda^m\frac{D(\lambda)}{\sqrt{1-\lambda}}\right] \text{Ry}^* , \tag{22}$$

where $D(\lambda)$ is defined in (20). Moreover, the energies of the $(0m0)$ states are very close to the energies of the respective MD ground states, as discussed below.

In order to illustrate the last point, we consider the lowest MD states attached to the $n=2$ Landau subband in the parabolic-band approximation, i.e., taking the total energy $\langle E\rangle=\langle K\rangle+\langle V\rangle$. For the (020) state

$$\langle E\rangle_{020}=5\gamma+\tfrac{1}{4}\gamma\lambda-\left[\frac{\gamma\lambda}{2\pi}\right]^{1/2}\left[\frac{(3\lambda^2-8\lambda+8)D(\lambda)}{4(1-\lambda)^{5/2}}+\frac{3(\lambda-2)}{(1-\lambda^2)}\right] \text{Ry}^* . \tag{23}$$

For the (110) state

$$\langle E\rangle_{110}=5\gamma+\tfrac{1}{4}\gamma\lambda+\left[\frac{\gamma\lambda}{2\pi}\right]^{1/2}\left[\frac{(7\lambda^3-30\lambda^2-24\lambda-16)D(\lambda)}{8(1-\lambda)^{7/2}}+\frac{7\lambda^2-4\lambda+12}{4(1-\lambda)^3}\right] \text{Ry}^* . \tag{24}$$

For the (200) state

$$\langle E\rangle_{200}=5\gamma+\tfrac{1}{4}\gamma\lambda-\left[\frac{\gamma\lambda}{2\pi}\right]^{1/2}\left[\frac{(41\lambda^4-112\lambda^3+240\lambda^2-128\lambda+64)D(\lambda)}{32(1-\lambda)^{9/2}}-\frac{23\lambda^3+42\lambda^2-8\lambda+48}{16(1-\lambda)^4}\right] \text{Ry}^* . \tag{25}$$

Minimizing the above energies one can calculate the corresponding binding energies $E^b_{NM\beta}=(\frac{5}{2}\gamma \text{ Ry}^*)-E_{NM\beta}$ (in Ry* units). For $\gamma=56.9$ (corresponding to $B=8$ T in InSb) we calculate $E^b_{200}=4.094$ Ry* $E^b_{110}=3.994$ Ry*, and $E^b_{020}=3.905$ Ry*. Thus, the energies of the above MD states are nearly the same. This is true also for MD states attached to higher Landau subbands, where the differences are expected to be even less. Consequently, we calculate the energies of the $(0m0)$ states [which are much simpler to compute, cf. Eqs. (23)–(25)], identifying them with those of the ground MD states belonging to the $n=m$ Landau subbands.

In Fig. 2 we show the binding energies (in Ry* units)

$$E^b_{0m0}=[\gamma(2m+1) \text{ Ry}^*]-E^{\text{var}}_{0m0} \tag{26}$$

calculated with the use of the variational procedure [based on Eqs. (21) and (22)] for the standard energy band (i.e., taking $\langle E\rangle=\langle K\rangle+\langle U\rangle$). It can be seen that the binding energies decrease with increasing Landau number $n=m$. This can be understood qualitatively by observing that higher MD states have progressively larger radii, so that the corresponding Coulomb energies (which are responsible for the electron binding) are progressively smaller. The double logarithmic plot of E^b_{0m0} versus γ are almost straight lines, which means that E^b_{0m0} is to a good approximation a power function of magnetic field.

In the actual comparison of the theory with experiment on InSb we calculate the MD energies using Eq. (12), which results from the three-level model with the approximation that $E-\langle U\rangle \ll \varepsilon_g+2\Delta/3$. This is a simpler procedure than the one used for calculating the Landau-level energies,[32] since the latter includes higher band contributions to k^2 terms. For this reason we calculate first the MD binding energies using Eq. (12) and the same model for the Landau-level energies. This amounts to putting $\langle U\rangle=0$ and $\langle K\rangle_{0m0}=\gamma(2m+1)$ Ry* is Eq. (12). Once the MD binding energies are calcu-

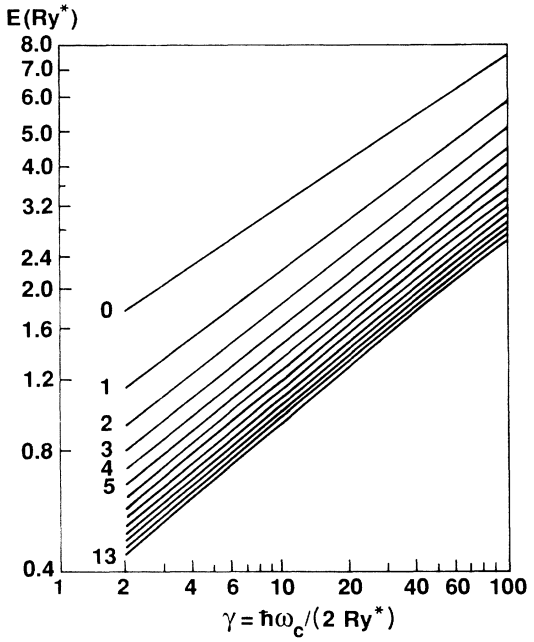

FIG. 2. Calculated binding energies of magnetodonor states attached to the consecutive Landau subbands $n=0,1,2,\ldots,13$ vs the parameter γ (for the parabolic energy band).

lated, they are subtracted from the Landau-level energies computed using the Pidgeon-Brown scheme. This gives the theoretical energies of the optical transitions between MD states.

D. Selection rules

Having chosen the trial functions of appropriate symmetry, one can calculate the selection rules for optical transitions between MD states (cf. Ref. 34). The main selection rules for a spherical energy band are quoted in Table I. They can be understood by keeping in mind that the MD problem with a scalar effective mass possesses a cylindrical symmetry. This symmetry is preserved in the Dingle gauge for the vector potential and it is reflected in the trial wave functions given in Eq. (15). When the spin is included, the projection of the total electron momentum on the magnetic field direction $j_z = M \pm \frac{1}{2}$ is a good quantum number. One can deduce the selection rules of Table I remembering that the photons of σ_L, σ_R, and π polarizations carry the values of $j_z = +1$, -1, 0, respectively. Complications of the band structure, such as nonsphericity and the lack of inversion symmetry, result in additional selection rules.[20,21] These are discussed in the next section.

As already mentioned in the Introduction, an emission or absorption of optic phonons breaks the selection rules for the free-electron magneto-optical transitions. This allows one to observe higher harmonics of cyclotron resonance, i.e., transitions with $\Delta n > 1$. Below we theoretically describe phonon-assisted magneto-optical transitions between MD states using wave functions given in Eq. (15).

A phonon-assisted magneto-optical transition is a two-quantum process, in which photon absorption is simultaneously accompanied by an emission of an optic phonon. We deal with electron-photon and electron-phonon interactions simultaneously perturbing the system. The transition probability of such a second-order process is given by

$$W_{\rm if} = \frac{2\pi}{\hbar} |M_{\rm if}|^2 \delta(E_f - E_i) , \tag{27}$$

where the matrix element is

$$M_{\rm if} = \sum_l \frac{\langle f|H_R|l\rangle\langle l|H_L|i\rangle}{E_l - E_i} + \sum_{l'} \frac{\langle f|H_L|l'\rangle\langle l'|H_R|i\rangle}{E_{l'} - E_i} . \tag{28}$$

The summation is over intermediate states and H_R and H_L denote the electron-photon and electron-phonon interactions, respectively. In the simplest scheme for the interband transitions we have $H_R = (e/m_0^*)\mathbf{A}'\cdot\mathbf{P}$, where $\mathbf{A}'$ is the vector potential of the radiation. The Fröhlich Hamiltonian is $H_L = (C/q)[b_q \exp(i\mathbf{q}\cdot\mathbf{r}) - b_q^\dagger \exp(-i\mathbf{q}\cdot\mathbf{r})]$, where $C^2 = (2\pi e^2\hbar\omega_L/V)(1/\kappa_\infty - 1/\kappa_0)$. The quantities κ_∞ and κ_0 are the high-frequency and static dielectric constants, $\mathbf{q}$ is the phonon wave vector, $\hbar\omega_L$ is the phonon energy, and b_q and $b_q^\dagger$ are the phonon annihilation and creation operators, respectively.

Equations (27) and (28) describe both the free-electron and MD phonon-assisted transitions. For MD transitions the matrix elements of H_R give the selection rules quoted in Table I. To focus the reader's attention, let us consider the matrix elements of H_L (for phonon emission) in the first term of Eq. (28), beginning with the ground MD state (000) and ending with the state $(NM\beta)$. We use the one-parameter trial functions, i.e., put in Eq. (15) $a = 1$. The calculation of the matrix elements can be separated into an integral over z involving the term $\exp(-iq_z z)$, and the corresponding integral over (ρ,ϕ). The integral over z couples the ground state to a state of arbitrary β. For $\beta = 0$ and 1 this is seen directly from Eqs. (16) and (17), the integral over ϕ and ρ,

$$F = \int \psi_{NM} e^{-iq_x x - iq_y y} \psi_{00} \rho \, d\rho \, d\phi , \tag{29}$$

where ψ_{NM} is the (ρ,ϕ) part of the trial functions (15), can be done explicitly, as shown below.

Writing $q_x x + q_y y = q_\perp \rho \cos\phi$, where $q_\perp^2 = q_x^2 + q_y^2$, and counting the angle ϕ from the vector $\mathbf{q}_\perp = (q_x, q_y)$, the integral over ϕ is

$$\frac{1}{2\pi}\int_{-\pi}^{\pi} e^{-iM\phi - iq_\perp\rho\cos\phi} d\phi = i^m J_m(-q_\perp\rho) , \tag{30}$$

where J_m is the Bessel function and $m = |M|$, as before. The remaining integral over ρ, containing the Bessel function, the Laguerre polynomial, the exponential, and the power function, can also be done analytically. The final result is

$$F = (-1)^N(-i)^m \left[\frac{N!}{(N+m)!}\right]^{1/2} t^{m/2} e^{-t} L_N^{N+m}(t) , \tag{31}$$

where $t = L^2 q_\perp^2/2$. The result shown in Eq. (31) is similar to that obtained for the phonon-assisted free-electron transitions with the use of the Landau (asymmetric) gauge for $\mathbf{A}$ (cf. Refs. 23 and 24). This is not surprising

TABLE I. Selection rules for the main magneto-optical transitions between donor states at high magnetic fields for various light polarizations. The symbols s, M, and N refer to the spin, angular momentum, and Landau quantum numbers, respectively. The symbol β is the number related to the quantized motion parallel to the magnetic field.

Polarization	Δs	ΔM	Δn	$\Delta\beta$
σ_L	0	+1	+1	0
	+1	0	0	±1
σ_R	0	−1	−1	0
	−1	0	0	±1
π	0	0	0	±1
	−1	+1	+1	0
	+1	−1	−1	0

since, by putting $a^2=1$ in the wave functions (15), we have tacitly assumed that the transverse MD motion is identical to the free-electron motion, and the final result for the transition probability should be gauge invariant.

The above results show that the Fröhlich electron-phonon interaction can couple the ground MD state (000) to an arbitrary MD state ($NM\beta$). In other words, an optic-phonon emission breaks the magneto-optical selection rules for the MD transitions, as it does for the free-electron transitions. The physical interpretation is that a momentum transfer due to the phonon emission breaks the cylinderical MD symmetry, and the angular-momentum selection rules of Table I cease to be valid.

The matrix element given in (29) can also be calculated analytically for the two-parameter MD functions given in (15), allowing for the variational adjustment of the transverse motion (the corresponding integrals can be found in Ref. 38). The final result is qualitatively similar to (31), but it now differs quantitatively from that for the phonon-assisted transitions.

The δ function in (27) involves the total energies of the initial and final states (including photons and phonons). We have $E_i=E_i^{\rm MD}+\hbar\omega$ and $E_f=E_f^{\rm MD}+\hbar\omega_L$. Energy conservation requires that $E_f-E_i=0$, which yields the resonance condition

$$\hbar\omega=E_f^{\rm MD}-E_i^{\rm MD}+\hbar\omega_L \ . \tag{32}$$

In the limit of $B\rightarrow 0$ the difference $E_f^{\rm MD}-E_i^{\rm MD}$ is practically zero, so that the phonon-assisted MD transition energies should converge to $\hbar\omega=\hbar\omega_L$, in a similar fashion to the phonon-assisted free-electron transitions between Landau levels. This is indeed observed experimentally, as will be shown in the following section.

It should be finally mentioned that in InSb-type semiconductors the probability of spin-flip transitions directly induced by optic phonons is low (although nonvanishing, cf. Ref. 39). For this reason, in phonon-assisted spin-flip transitions (cf. the transition $2'^-$ in Figs. 1, 5, and 7) the spin reversal is likely to occur due to the spin-photon interaction rather than the spin-phonon part of the matrix element (28) (cf. Ref. 26).

IV. RESULTS AND DISCUSSION

In Fig. 3 we show the energies of the observed free-electron and MD transitions as a function of the magnetic field strength, together with the energies calculated using the Pidgeon and Brown model.[32] It can be seen that some energies correspond to simple and others to phonon-assisted excitations. This correlation of the theory with experiment served as a basis of our transition assignments. The free-electron transition $0^+\rightarrow 2^+$, $0^+\rightarrow 2^-$, and $0^+\rightarrow 3^+$ (where n^+ and n^- denote the Landau levels n with spin-up and spin-down, respectively) and the associated MD transitions for these levels have been observed previously by Grisar *et al.*[20] For our field orientation $\mathbf{B}\|[111]$ and the light polarization $\mathbf{E}\perp\mathbf{B}$ the $2\omega_c$ ($0^+\rightarrow 2^+$) and the $2\omega_c+\omega_s$ ($0^+\rightarrow 2^-$) transitions are allowed due to the inversion asymmetry of InSb.[21] The observed transition $3\omega_c$, however, is not allowed for this field orientation. The same difficulty was

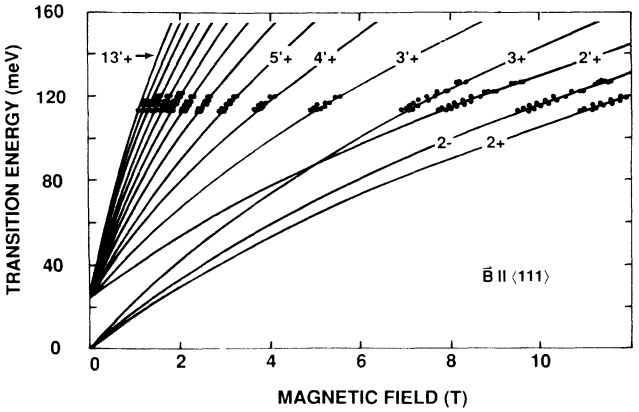

FIG. 3. Energies of the observed magnetodonor and Landau-level transitions vs magnetic field (solid dots). The solid lines indicate the calculated energies of Landau-level transitions for simple excitations (converging to $\hbar\omega=0$), and phonon-assisted excitations (converging to $\hbar\omega=\hbar\omega_L$).

encountered by Favrot *et al.*,[22] who observed the transition $2\omega_c$ for $\mathbf{B}\|[001]$, which is not allowed. The current (not confirmed) interpretation is that such forbidden transitions become allowed by the assistance of shallow impurities in the same way as the phonon-assisted ones.[40] Judging by the doublet structure shown in Fig. 1, the corresponding donor-shifted transitions are allowed for the same reasons.

Figure 4 shows our data for transitions to higher final states for which the distinction between free-electron and MD excitations was presently possible. The phonon assistance provides a unique opportunity to investigate high excited states of the magneto-Coulomb system. We have been able to observe and describe transitions to final MD states attached to the Landau subbands n up to $n=13$. In Fig. 5 and 6 we show the observed and calculated energies of Landau-level and MD transitions. The transi-

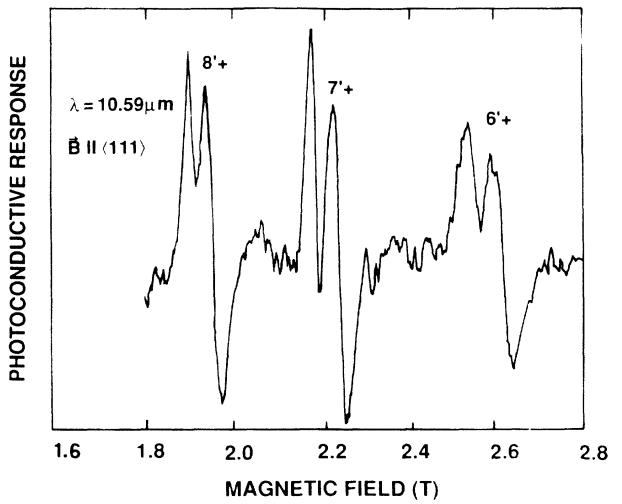

FIG. 4. Photoconductive response vs magnetic field showing the Landau-level–magnetodonor doublet structure for higher quantum numbers.

tions labeled by the primed numbers are the phonon-assisted excitations. The solid lines for the Landau-level transitions in Figs. 5 and 6 were calculated using the Pidgeon-Brown model with the following band parameters: $\varepsilon_g = 235.2$ meV, $E_p = 23.2$ eV, $\Delta = 0.803$ eV, $\gamma_1 = 3.25$, $\gamma_2 = -0.2$, $\gamma_3 = 0.9$, $\kappa = -1.3$, $F = -0.2$, $q = 0.0$, and $N_1 = -0.55$. This corresponds to the band-edge values of $m_0^* = 0.0136 m_0$ and $g_0^* = -51.1$. These parameters describe well also other magneto-optical data taken on InSb (cf. Ref. 41). The phonon-assisted LL transition energies were obtained by adding the LO optic-phonon energy $\hbar\omega_L = 24.4$ meV to the calculated free-electron energies.

As indicated in the inset of Fig. 5, the shift between the Landau-level and MD transitions is due to the fact that, with increasing n, the binding energies of the corresponding MD states become smaller. The dashed lines for the MD transitions in Figs. 5 and 6 have been calculated by adding the corresponding shifts: $\delta(n) = E^b_{\rm MD}(n) - E^b_{\rm MD}(0)$ to the Landau-level transition energies. This procedure has been discussed in the previous section. In order to get the best fit to the data we used the value 1 Ry$^* = 0.65$ meV. With the above-quoted value of m_0^* it corresponds to the static dielectric constant $\kappa_0 = 16.9$, which is very reasonable (cf. discussion in Ref. 42). The agreement between experiment and theory is very good (it is seen more clearly in Fig. 7 for the $2'^+$ transition at one laser wavelength).

Our highest resolution data revealed two additional resonances on the lower field side, as shown in Fig. 7 for the $0^+ \rightarrow 2^+$ phonon-assisted excitations. The additional resonances are present in the phonon-assisted as well as the ordinary MD transitions. This suggests that the resonances are due to additional selection rules caused by the band-structure complications rather than the phonons. The transitions shown in Fig. 7 have been identified as originating from the MD ground state (000^+) to excited MD states associated with the 2^+ Landau subband. The corresponding selection rules have been calculated by Wlasak.[43] The main transition ($000^+ \rightarrow 200^+$) [or the transition ($000^+ \rightarrow (020^+$) having almost the same ener-

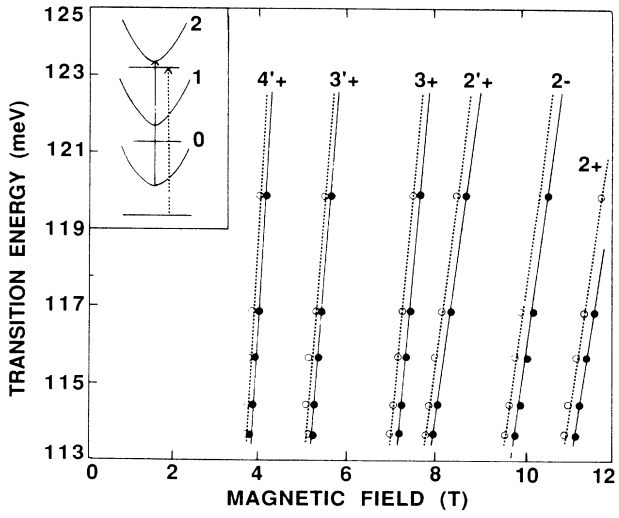

FIG. 5. Energies of the free-electron (solid circles) and magnetodonor (open circles) transitions vs magnetic field for the Landau quantum numbers 1–4. Primed numbers indicate phonon-assisted transitions. The solid lines were calculated using the Pidgeon-Brown model and the dashed lines were obtained by adding the calculated donor shifts. The inset shows a schematic diagram of the free-electron (solid arrow) and associated magnetodonor (dashed arrow) transitions.

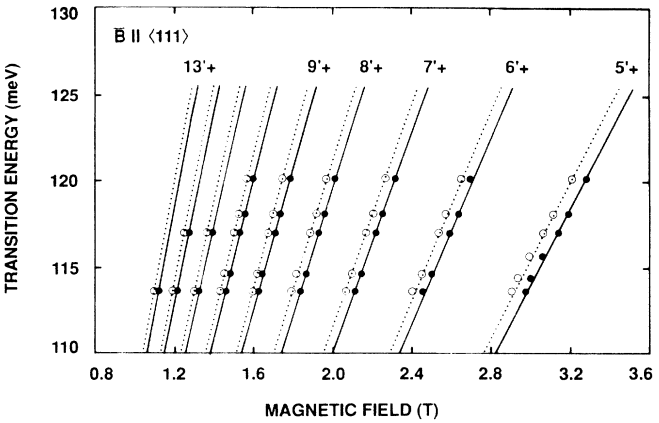

FIG. 6. Energies of the free-electron (solid circles) and magnetodonor (open circles) transitions vs magnetic field for the Landau quantum numbers 5–13. The solid lines were calculated using the Pidgeon-Brown model and the dashed lines were obtained by adding the calculated donor shifts.

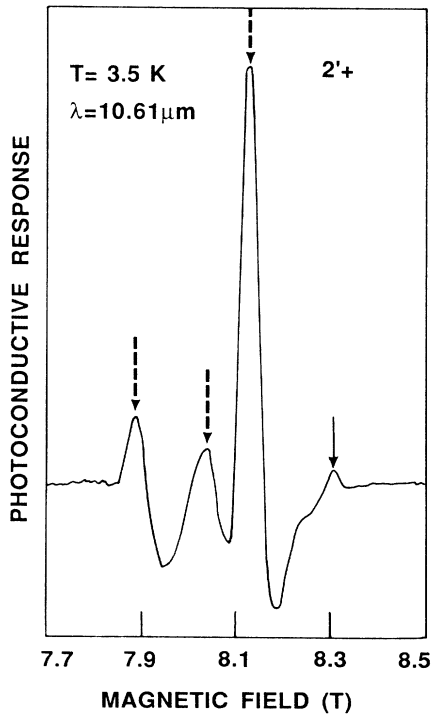

FIG. 7. High-resolution magneto-optical spectrum for the phonon-assisted free-electron $0^+ \rightarrow 2^+$ transition (solid arrow), and the (000^+)$\rightarrow$(200^+), (000^+)$\rightarrow$($2\bar{3}0^+$), (000^+)$\rightarrow$($2\bar{1}1^+$) MD transitions (from left to right). The calculated field positions for the transitions are indicated by the arrows (see text).

gy, cf. discussion in Sec. III C] is possible due to inversion asymmetry. The weaker transitions are possible due to band warping. The best theoretical fit to the middle transition has been obtained for the final MD state $(2\bar{3}0)$ (the calculated binding energy is $E_b=1.80$ meV at $B=8$ T), but we cannot exclude the states $(2\bar{2}0)$ ($E_b=2.07$ meV) and $(2\bar{1}0)$ ($E_b=2.31$ meV) as possible final states. For the lowest field transition in Fig. 7 the best fit is obtained for the final MD state $(2\bar{2}1)$ ($E_b=0.626$ meV), but again we cannot exclude the nearby states (111) ($E_b=0.657$ meV) and (021) ($E_b=0.675$ meV). All of the above binding energies have been calculated for $B=8$ T. The weaker resonances require further investigation concerning their dependence on light polarization orientation of the magnetic field, and precise assignment of the final MD states.

The theoretical description presented above has aimed to treat consistently the high excited MD states in a workable fashion, which required the four simplifications discussed below. (1) In order to arrive at the simple nonparabolic formula given in Eq. (12) for the variational MD energies from the $\mathbf{P}\cdot\mathbf{p}$ theory (9) within the three-level model, we have neglected the commutators $[p,U]$ and assumed that $E-\langle U\rangle<\varepsilon_g+2\Delta/3$. This approximation is known to affect the ground state (000) and can lead to a few percent error in the energy estimations (it lowers the ground state, increasing the binding energy at high fields, cf. Ref. 44). (2) We have neglected central-cell corrections due to the short-range component of the donor potential. This, again, affects mostly the MD ground-state energy. The exact chemical nature of the donors in our InSb samples is not known. (3) We have identified energies of the ground MD states ($N00$) with the slightly higher energies of the ($0m0$) states (for $m=N=2,3,4,\ldots$), since the latter are much easier to calculate. This also introduces a few percent error in the energy estimations. On the other hand, we do not really know whether the phonon-assisted transitions occur to the final ($N00$) or ($0m0$) MD states. (4) In the energy estimations we have used the one-parameter variational functions of the Wallis and Bowlden[37] type, which are valid for the $\gamma>10$ range of the magnetic field intensities. This criterion is not well satisfied for the transitions to the highest MD levels, which occur at lower magnetic fields (cf. Fig. 6). This leads to slight underestimations of the binding MD energies at low fields.

All of the above approximations amount to a few percent of the binding energies. The latter are small compared to the transitions energies we observe, so that a high theoretical precision is not necessary. The accepted values of the effective rydberg for donors in InSb range from 0.6 to 0.7 meV and our overall good fit to the data with the value 1 Ry$^*=0.65$ meV should be considered a success.

In summary, we have observed and described optical transitions between magnetodonor states in InSb, assisted by the emission of longitudinal optic phonons. The observation of the doublet structure due to magnetodonor and Landau-level transitions for high excited states of the system have been made possible by combining photoconductive detection with magnetic field modulation. The phonon assistance breaks the selection rules and allows for the opportunity of studying high excited states of an electron subjected to simultaneous Coulomb and magnetic field interactions. This is of direct interest to semiconductor physics, atomic physics, and astrophysics.

ACKNOWLEDGMENTS

We are grateful to Dr. M. Kubisa of the Institute of Physics in Warsaw for elucidating discussions concerning the theoretical aspects of this work. This work was supported in part by National Science Foundation Grant No. DMR-86-17823.

*Permanent address: Institute of Physics, Polish Academy of Sciences, PL-02-668, Warsaw, Poland.

[1]R. W. Keyes and R. J. Sladek, Phys. Chem. Solids **1**, 143 (1956).
[2]Y. Yafet, R. W. Keyes, and E. N. Adams, Phys. Chem. Solids **1**, 137 (1956).
[3]R. Kaplan, Phys. Rev. **181**, 1154 (1969).
[4]B. D. McCombe and R. J. Wagner, Phys. Rev. B **6**, 1285 (1971).
[5]B. D. McCombe and R. Kaplan, Phys. Rev. Lett. **21**, 756 (1968); B. D. McCombe, Phys. Rev. **181**, 1206 (1969).
[6]G. E. Stillman, C. M. Wolfe, and J. O. Dimmock, Solid State Commun. **7**, 921 (1969).
[7]W. Zawadzki and J. Wlasak, J. Phys. C **17**, 2505 (1984).
[8]F. Kuchar, R. Kaplan, R. J. Wagner, R. A. Cooke, R. A. Stradling, and P. Vogl, J. Phys. C **17**, 6403 (1984).
[9]E. W. Fenton and R. R. Haering, Phys. Rev. **159**, 593 (1967).
[10]J. L. Robert, A. Raymond, R. L. Aulombard, and C. Bousquet, Philos. Mag. B **42**, 1003 (1980).
[11]N. C. Jarosik, B. D. McCombe, B. V. Shannabrook, J. Comas, J. Ralston, and G. Wicks, Phys. Rev. Lett. **54**, 1283 (1985).
[12]W. Zawadzki, M. Kubisa, A. Raymond, J. L. Robert, and J. P. Andre, Phys. Rev. B **36**, 9297 (1987).
[13]R. H. Garstang, Rep. Prog. Phys. **40**, 105 (1977); G. Wunner and H. Ruder, Astrophys. J. **242**, 828 (1980).
[14]G. Wunner, W. Rösner, H. Herold, and H. Ruder, Astron. Astrophys. **149**, 102 (1985).
[15]G. L. Surmelian and R. F. O'Connell, Astrophys. **190**, 741 (1974).
[16]H. Ruder, G. Wunner, H. Herold, and J. Trümper, Phys. Rev. Lett. **46**, 1700 (1981).
[17]G. Wunner, H. Ruder, H. Herold, and W. Schmitt, Astron. Astrophys. **117**, 156 (1983).
[18]W. Rösner, G. Wunner, H. Herold, and H. Ruder, J. Phys. B **17**, 29 (1984).
[19]W. Zawadzki, in *Landau Level Spectroscopy*, edited by G. Landwehr and E. I. Rashba (North-Holland, Amsterdam, in press).
[20]R. Grisar, H. Wachernig, G. Bauer, J. Wlasak, J. Kowalski, and W. Zawadzki, Phys. Rev. B **18**, 4355 (1978).
[21]M. H. Weiler, R. L. Aggarwal, and B. Lax, Phys. Rev. B **17**, 3269 (1978).

[22]G. Favrot, R. L. Aggarwal, and B. Lax, Solid State Commun. **18**, 577 (1976).
[23]R. C. Enck, A. L. Saleh, and H. Y. Fan, Phys. Rev. **182**, 790 (1969).
[24]F. G. Bass and I. B. Levinson, Zh. Eksp. Teor. Fiz. **69**, 916 (1965) [Sov. Phys.—JETP **22**, 635 (1966)].
[25]M. W. Goodwin and D. G. Seiler, Phys. Rev. B **27**, 3451 (1983).
[26]W. Zawadzki, R. Grisar, H. Wachernig, and G. Bauer, Solid State Commun. **25**, 775 (1978).
[27]R. Kaplan and R. F. Wallis, Phys. Rev. Lett. **20**, 1499 (1968).
[28]The first results of this work have been reported in C. L. Littler, W. Zawadzki, M. R. Loloee, X. N. Song, and D. G. Seiler, Phys. Rev. Lett. **63**, 2845 (1989).
[29]S. Huant, L. C. Brunel, M. Baj, L. Dmowski, N. Coron, and G. Dambier, Solid State Commun. **54**, 131 (1985).
[30]C. L. Littler and D. G. Seiler, J. Appl. Phys. **60**, 261 (1986).
[31]H. Kalhert and D. G. Seiler, Rev. Sci. Instrum. **48**, 1017 (1977).
[32]C. R. Pidgeon and R. N. Brown, Phys. Rev. **146**, 575 (1966). The paper contains two erroneous signs in the matrix for the *b*-set levels (cf. Refs. 20 and 21).
[33]D. M. Larsen, J. Phys. Chem. Solids **29**, 271 (1968).
[34]W. Zawadzki and J. Wlasak, in *Theoretical Aspects and New Developments in Magneto-Optics,* edited by J. T. Devreese (Plenum, New York, 1980), p. 347. The formulas for the trial energy averages in this paper contain typographical errors.
[35]E. O. Kane, Phys. Chem. Solids **1**, 249 (1957).
[36]R. Bowers and Y. Yafet, Phys. Rev. **115**, 1165 (1959).
[37]R. F. Wallis and H. J. Bowlden, Phys. Chem. Solids **7**, 78 (1958).
[38]A. P. Prudnikov, Yu. A. Brychkov, and O. I. Marichev, *Integrals and Series: Special Functions* (Nauka, Moscow, 1983, in Russian).
[39]W. Zawadzki, G. Bauer, W. Racek, and H. Kahlert, Phys. Rev. Lett. **35**, 1098 (1975).
[40]W. Zawadzki, in *Narrow Gap Semiconductors. Physics and Applications,* Vol. 133 of *Lecture Notes in Physics,* edited by W. Zawadzki (Springer, Berlin, 1980), p. 85.
[41]C. L. Littler, D. G. Seiler, R. Kaplan, and R. J. Wagner, Phys. Rev. B **27**, 7473 (1983).
[42]J. R. Dixon, Jr. and J. K. Furdyna, Solid State Commun. **35**, 195 (1980).
[43]J. Wlasak J. Phys. C **18**, 4001 (1985); **19**, 4143 (1986).
[44]R. Kaplan, in Ref. 40, p. 138.